

# Performance Analysis of Multi-Relay Assisted IoT Networks in Mixed Fading Environments

Jiajia Huang<sup>1,\*</sup>, Fusheng Wei<sup>1</sup>, Jingming Zhao<sup>1</sup>, and Huakun Que<sup>1</sup>

<sup>1</sup>Guangdong Power Grid Co., Ltd, Guangzhou, China

## Abstract

This study studies a multi-relay assisted Internet of Things (IoT) network within the context of mixed fading environments. Here, data transmission from the source to the destination is assisted through multiple decode-and-forward (DF) relays. In particular, this work revolves around mixed fading environments, characterized by the first-hop relaying links conforming to a uniform distribution while the second-hop relaying links exhibit Rayleigh fading. To enhance the overall efficacy of the network, we introduce two relay selection criteria. Specifically, the first criterion entails an optimal selection process hinging on the identification of the most proficient relay. This selection relies upon the channel parameters of dual-hop relaying links. In contrast, the second criterion adopts a sub-optimal selection approach by singling out the optimal relay solely based on the channel parameters of the second-hop relaying links. The performance evaluation of the two aforementioned relay selection criteria entails the derivation of analytical expressions governing the system outage probability. To validate the theoretical works presented in this research, we supplement our analysis with simulation results. Notably, our findings underscore the efficacy of augmenting network performance by augmenting the number of relays within the network topology, even in complicated mixed fading environments.

Received on 26 August 2023; accepted on 16 November 2023; published on 22 November 2023

**Keywords:** Multi-relay, IoT, outage probability, mixed fading

Copyright © 2023 Jiajia Huang *et al.*, licensed to EAI. This is an open access article distributed under the terms of the [Creative Commons Attribution license](#), which permits unlimited use, distribution and reproduction in any medium so long as the original work is properly cited.

doi:10.4108/eetsis.3798

## 1. Introduction

The evolution of Internet of Things (IoT) networks has been profoundly catalyzed by significant advancements in both mobile communication and edge computing [1–4]. The proliferation of mobile communication technologies, such as the fourth-generation (4G) and fifth-generation (5G), has provided the foundation for seamless connectivity and data exchange across diverse IoT devices [5–8]. These technologies offer higher bandwidth, lower latency, and increased capacity, allowing IoT devices to transmit and receive data more efficiently and reliably. Additionally, the rise of edge computing has revolutionized the way IoT networks function. By enabling data processing and analysis to occur closer to the data source, at the network's edge, edge computing reduces the strain on centralized cloud resources and minimizes latency [9–11]. This

paradigm shift not only accelerates real-time decision-making but also enhances privacy and security by processing sensitive data locally [12–14]. Consequently, the synergy between advanced mobile communication and edge computing has propelled the development of IoT networks, fostering innovation across industries by enabling smarter, more interconnected devices and systems [15–18].

To enhance the performance of IoT networks, relaying protocols have been proposed, which play a pivotal role in enhancing the efficiency and reliability of communication systems, particularly in scenarios where signal degradation and coverage limitations are prevalent [19–21]. Among the notable relaying protocols are decode-and-forward, amplify-and-forward, and denoise-and-forward [22–25]. The decode-and-forward protocol involves the intermediate relay decoding the received signal from the source and subsequently re-encoding it for transmission to the destination. This approach leverages error correction coding

\*Corresponding author. Email: [Huangjiajia.eecs@hotmail.com](mailto:Huangjiajia.eecs@hotmail.com)

to mitigate errors and enhance overall reliability [26–28]. Amplify-and-forward, on the other hand, focuses on the relay amplifying the received signal before transmitting it to the destination. While it avoids the need for decoding, it is susceptible to noise and amplification distortion. Denoise-and-forward stands out by employing advanced signal processing techniques at the relay to suppress noise before transmitting to the destination. This protocol particularly excels in scenarios with high noise levels [29–31]. Each of these relaying protocols presents a distinct trade-off between complexity, performance, and practical implementation considerations, making their selection contingent on the specific communication environment and network requirements.

The integration of multiple relays into communication systems offers a host of advantages that significantly augment system performance and robustness [32–34]. One of the foremost benefits lies in the reduction of system outage probability and symbol error rate. By employing multiple relays, the network gains improved spatial diversity, effectively mitigating the adverse effects of fading and signal attenuation [35–37]. The increase in diversity order translates to enhanced reliability as the likelihood of simultaneous signal degradation across all relays diminishes, resulting in more consistent and reliable data transmission. The collaborative efforts of multiple relays in forwarding signals amplify the received signal strength at the destination, thereby bolstering the signal-to-noise ratio (SNR). This collective reinforcement, in turn, leads to reduced error rates and better overall communication quality [38–41]. In essence, the incorporation of multiple relays harnesses the inherent diversity within the communication environment, transforming it into a valuable asset that elevates the system performance and reinforces the seamless connectivity.

Motivated by the above literature review, this work investigates a multi-relay assisted IoT network within the context of mixed fading environments. In this setting, data transmission from the source to destination is assisted by multiple decode-and-forward relays. In particular, our investigation centers on mixed fading environments, characterized by the first-hop relaying links adhering to a uniform distribution, while the second-hop relaying links are subject to Rayleigh fading. To enhance the overall efficiency of the network, we introduce two relay selection criteria. Specifically, the first criterion involves an optimal selection process pivoting on the identification of the most proficient relay, relying on the channel parameters of dual-hop relaying links. In contrast, the second criterion adopts a sub-optimal selection approach, singling out the optimal relay based solely on the channel parameters of the second-hop relaying links. Evaluating the performance of these relay selection

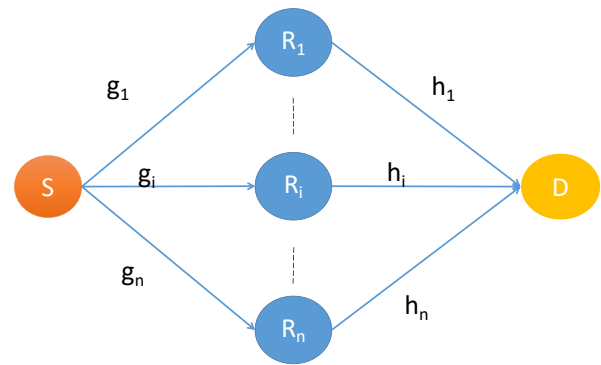


**Figure 1.** System model of multi-relay assisted IoT Networks in mixed fading environments.

criteria necessitates deriving analytical expressions governing the system overall outage probability. To validate the theoretical foundations presented in this research, we complement our analysis with simulation results, notably underscoring the efficacy of improving network performance by increasing the number of relays within the network topology, even in complicated mixed fading environments.

## 2. System Model of Multi-relay assisted IoT network structure

Fig. 1 shows the system model of multi-relay assisted IoT networks in mixed fading environments, where  $S$  is the transmit node,  $D$  is the receive node. Between  $S$  and  $D$ , there are  $n$  decode-and-forward (DF) relays denoted by  $\{R_i | i \in [1, n]\}$ , where  $n$  is the total number of relays. Through establishing multiple relay nodes, the network topology with redundant paths can be formed. When a node fails or the signal quality decreases, other nodes can take over signal transmission to ensure continuity of communication, reduce the risk of signal interruption, and improve communication reliability.

Let  $x_S$  be the transmitted signal, and then the received signal at the  $i$ -th relay node can be expressed as

$$y_{R_i} = g_i * \sqrt{P} * x_S + n_R, \quad (1)$$

where  $n_R \sim CN(0, \sigma^2)$  is the white noise,  $P$  is the transmit power at the source, and  $g_i$  is the wireless channel from  $S$  to  $R_i$  where its probability density function (PDF) is expressed as

$$f_{|g_i|^2}(u) = \begin{cases} \frac{1}{\theta_b - \theta_a}, & \text{If } u \in [\theta_a, \theta_b] \\ 0, & \text{Otherwise} \end{cases} \quad (2)$$

From  $y_{R_i}$ , the relay  $R_i$  can decode the transmitted signal, and then send the decoded signal to the destination  $D$ . Accordingly, the received signal at  $D$  is,

$$y_D = h_i * \sqrt{P} * x_S + n_D, \quad (3)$$

where  $n_D \sim CN(0, \sigma^2)$  is the white noise,  $h_i$  is the wireless channel from  $R_i$  to  $D$  and its probability density function (PDF) is expressed as

$$f_{|h_i|^2}(v) = \begin{cases} \frac{1}{\alpha} e^{-\frac{v}{\alpha}}, & \text{If } v > 0 \\ 0, & \text{Otherwise} \end{cases} \quad (4)$$

From the above equations, we can write the end-to-end received signal-to-noise ratio (SNR) with the  $i$ -th relay as,

$$\text{SNR}_{e2e,i} = \frac{P}{\sigma^2} \min(|h_i|^2, |g_i|^2). \quad (5)$$

### 3. System optimization and performance analysis

#### 3.1. Relay selection

To enhance the network performance, we can choose one best relay among  $n$  ones to assist the data transmission from  $S$  to  $D$ . When the channel state information (CSI) of dual-hop relaying links is available, we can perform the relay selection according to the following criterion,

$$n^* = \arg \max_{1 \leq i \leq n} \min(|g_i|^2, |h_i|^2). \quad (6)$$

Note that this relay selection process based on dual-hop relaying links involves a strategic approach to optimize the network performance, which aims to identify the most suitable relay for the data transmission by evaluating both fading conditions of the relay channels and ensuing signal quality. The selected relay, denoted as  $R_{n^*}$ , is determined by the relay index  $i$  that maximizes the minimum value between the squared magnitudes of the corresponding dual-hop relaying links  $g_i$  and  $h_i$ . By employing this selection criterion, the system seeks to strike a balance between the various relay options, considering both the quality of the individual relaying links and their collective impact on the data transmission reliability. This criterion ensures an optimal relay choice that capitalizes on the available resources and the network overall resilience against fading effects.

When only the CSI of the second-hop relaying links is available, we can perform the relay selection according to the following criterion,

$$n^* = \arg \max_{1 \leq i \leq n} |h_i|^2. \quad (7)$$

Note that the above partial selection criterion, rooted in the second-hop relaying links, offers a pragmatic strategy for optimizing the relay selection within the network. In this criterion, the selected relay  $R_{n^*}$  focuses exclusively on the squared magnitude of the second-hop relaying links  $h_i$  across the available relay

options indexed from 1 to  $n$ . By selecting the relay index  $i$  that maximizes this criterion, the system selects the relay with the strongest second-hop relaying link, thereby enhancing the signal quality during the second-hop data transmission. This criterion is particularly beneficial in scenarios where the second-hop relaying links are more indicative of improved transmission conditions, enabling a sub-optimal yet efficient relay choice. Through this criterion, the network can efficiently capitalize on the favorable aspects of second-hop relaying links to bolster the overall communication reliability.

#### 3.2. Outage probability analysis

The outage probability of the data transmission from  $S$  to  $D$  associated with the  $i$ -th relay can be described as,

$$P_{out,i} = \Pr(\text{SNR}_{e2e,i} < Y_{th}), \quad (8)$$

where  $Y_{th}$  is the threshold of targeted SNR. We firstly derive the analytical expression of outage probability when there is only one relay. Specifically, from the expression of  $\text{SNR}_{e2e,i}$ , we can re-write  $P_{out,i}$  as

$$P_{out,i} = \Pr\left(\min(|g_i|^2, |h_i|^2) < \frac{Y_{th}\sigma^2}{P}\right), \quad (9)$$

$$= 1 - \Pr\left(\min(|g_i|^2, |h_i|^2) > \frac{Y_{th}\sigma^2}{P}\right). \quad (10)$$

According to the distribution of  $|g_i|^2$  and  $|h_i|^2$ ,  $P_{out,i}$  can be derived as

$$P_{out,i} = 1 - \left(1 - \Pr\left(|g_i|^2 < \frac{Y_{th}\sigma^2}{P}\right)\right) \left(1 - \Pr\left(|h_i|^2 < \frac{Y_{th}\sigma^2}{P}\right)\right), \quad (11)$$

$$= 1 - \left(1 - \int_{\theta_a}^{\frac{Y_{th}\sigma^2}{P}} \frac{1}{\theta_b - \theta_a} du\right) \left(1 - \int_0^{\frac{Y_{th}\sigma^2}{P}} \frac{1}{\alpha} e^{-\frac{v}{\alpha}} dv\right), \quad (12)$$

$$= 1 - \left(1 - \frac{\frac{Y_{th}\sigma^2}{P} - \theta_a}{\theta_b - \theta_a}\right) e^{-\frac{Y_{th}\sigma^2}{P\alpha}}, \quad (13)$$

where  $\theta_a < \frac{Y_{th}\sigma^2}{P} < \theta_b$ .

From the above analytical outage probability of the system with only one relay, we proceed to derive the analytical outage probability with multiple relays. For criterion I performed in (6), the system outage probability can be expressed as,

$$P_{I,out} = \Pr\left(\text{SNR}_{e2e,n^*} < Y_{th}\right), \quad (14)$$

$$= \Pr\left(\min(|g_{n^*}|^2, |h_{n^*}|^2) < \frac{Y_{th}\sigma^2}{P}\right). \quad (15)$$

Due to the independence between the dual-hop relaying links, we can further write  $P_{I,out}$  as

$$P_{I,out} = 1 - \left( 1 - \Pr \left( |g_{n^*}|^2 < \frac{Y_{th}\sigma^2}{P} \right) \right) \times \left( 1 - \Pr \left( |h_{n^*}|^2 < \frac{Y_{th}\sigma^2}{P} \right) \right). \quad (16)$$

As  $n^* = \arg \max_{1 \leq i \leq n} \min(|g_i|^2, |h_i|^2)$ , we can write the analytical form of  $P_{out}$  from the theory of order statistics as

$$P_{I,out} = \left( 1 - \left( 1 - \frac{Y_{th}\sigma^2}{\theta_b - \theta_a} \right) e^{-\frac{Y_{th}\sigma^2}{P\alpha}} \right)^n. \quad (17)$$

On the other hand, when we use criterion II in (7) to choose the best relay to assist the data transmission, we should firstly analyze the distribution of  $|h_{n^*}|^2$  before deriving the analytical expression for the system outage probability. In particular, the distribution of  $|h_{n^*}|^2$  can be derived as

$$F_{|h_{n^*}|^2}(v) = \Pr(|h_{n^*}|^2 < v), \quad (18)$$

$$= \Pr(|h_1|^2 < v) \cdot \Pr(|h_2|^2 < v) \cdots \Pr(|h_n|^2 < v), \quad (19)$$

$$= \sum_{i=0}^n (-1)^i \binom{n}{i} e^{-\frac{iv}{\alpha}}, \quad (20)$$

where  $n^* = \arg \max_{1 \leq i \leq n} (|h_i|^2)$  is applied. From the above distribution of  $|h_{n^*}|^2$ , we can readily derive the analytical expression of outage probability for criterion II as,

$$P_{out,II} = 1 - \left( 1 - \frac{Y_{th}\sigma^2}{\theta_b - \theta_a} \right) \left( 1 - \sum_{i=0}^n (-1)^i \binom{n}{i} e^{-\frac{iY_{th}\sigma^2}{P\alpha}} \right). \quad (21)$$

## 4. Experimental results and discussions

In this section, we present the simulation results to validate the analytical findings. Specifically, we will analyze the impact of network parameters such as  $P$ ,  $Y_{th}$ ,  $\alpha$ , and  $n$  in the following experiments to verify the analytical results. The experiments in this section are divided into two parts, whereas the first part focuses on the IoT with a single relay, while the second part examines the IoT with multiple relays. The parameters  $\theta_a$  and  $\theta_b$  are set to 0 and 100, respectively, and  $\sigma^2$  is set to 3.

### 4.1. Outage probability of the system with $n = 1$ .

This part demonstrates the impact of network parameters on the system performance, when there is only

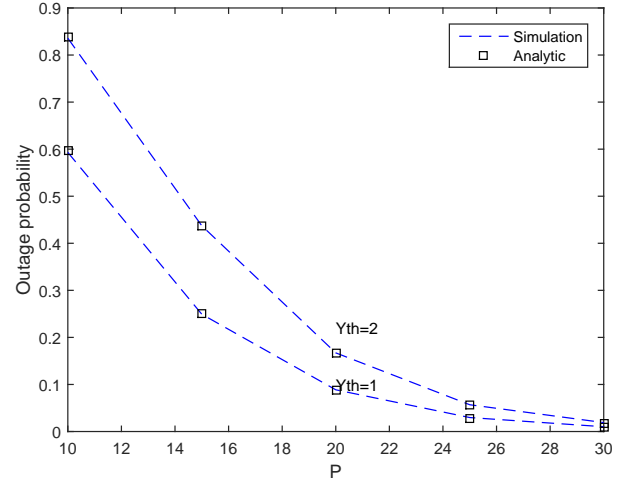


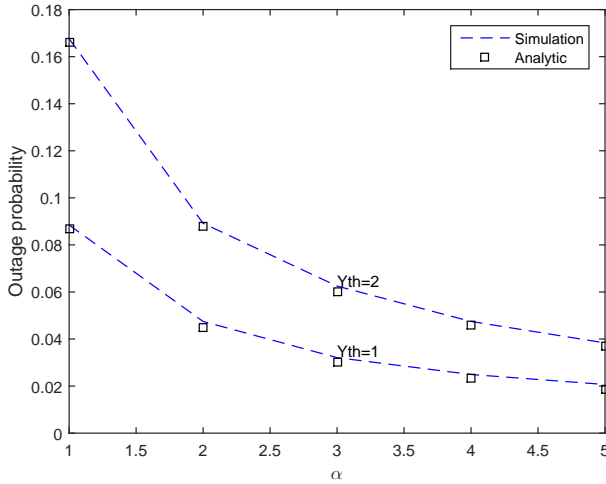
**Figure 2.** System outage probability with  $n = 1$  versus  $P$  and  $Y_{th}$ .

one relay with  $n = 1$ . In the first experiment, we set  $\alpha = 1$ ,  $P \in [10, 15, 20, 25, 30]$ , and  $Y_{th} \in [1.0, 2.0]$ . The experimental results are shown in Fig. 2 and Table 1. As depicted in Fig. 2 and Table 1, one can observe that the simulation and analytical results exhibit similar values for various values of  $Y_{th}$  and  $P$ . For instance, when  $Y_{th} = 1.0$  and  $P = 10\text{dB}$ , the simulation result is 0.5959, whereas the analytical result is 0.5971, yielding a difference of only 0.0012. Similarly, for  $Y_{th} = 2.0$  and  $P = 30\text{dB}$ , the simulation result is 0.0190, whereas the analytical result is 0.0186, yielding a difference of only 0.0004. Based on these findings, it can be concluded that the simulation results validate the analytical results, indicating the accuracy of the derived analytical outage probability. Moreover, there are two curves in Fig. 2 corresponding to two distinct values of  $Y_{th}$ , namely  $Y_{th} = 1.0$  and  $Y_{th} = 2.0$ . The curve associated with  $Y_{th} = 2.0$  lies above the curve with  $Y_{th} = 1.0$ , as a smaller threshold indicates an increased delay tolerance, thereby enhancing the system performance. In further, the results for both curves demonstrate that as  $P$  increases, the system outage probability decreases. This outcome signifies that a higher value of  $P$  can enhance the transmission capability for the considered system.

In the second experiment, we set  $P = 20\text{dB}$ ,  $\alpha \in [1, 2, 3, 4, 5]$ , and  $Y_{th} \in [1.0, 2.0]$ . In Table 2 and Fig. 3, we present the experimental results for the system with respect to  $Y_{th}$  and  $\alpha$ . As shown in Table 2 and Fig. 3, one can find that the simulation and analytical results yield similar values for different values of  $Y_{th}$  and  $\alpha$ . For instance, when  $Y_{th} = 1.0$  and  $\alpha = 1$ , the simulation result is 0.0885, while the analytical result is 0.0869, resulting in a difference of only 0.0016. Similarly, when  $Y_{th} = 2.0$  and  $\alpha = 5$ , the simulation result is 0.0384,

**Table 1.** Numerical outage probability with  $n = 1$  versus  $P$  and  $Y_{th}$ .

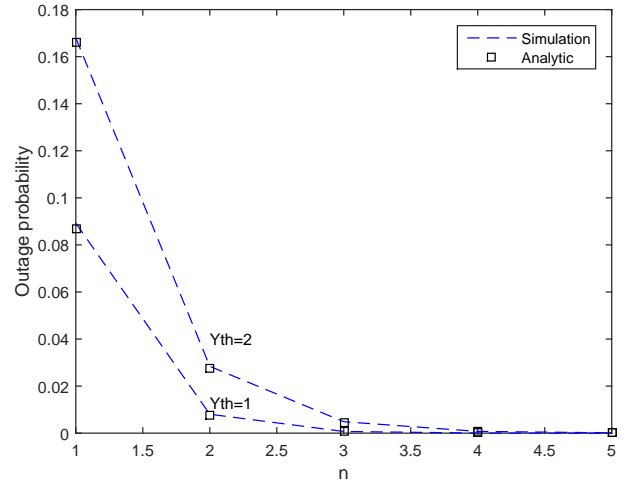
Methods	$Y_{th}$	$P/dB$				
		10	15	20	25	30
Simulation	1.0	0.5959	0.2528	0.0901	0.0298	0.0101
	2.0	0.8365	0.4368	0.1675	0.0564	0.0190
Analysis	1.0	0.5971	0.2498	0.0869	0.0283	0.0090
	2.0	0.8377	0.4372	0.1662	0.0559	0.00186

**Figure 3.** System outage probability with  $n = 1$  versus  $\alpha$  and  $Y_{th}$ .

while the analytical result is 0.0371, resulting in a difference of only 0.0013. Based on these findings, it can be concluded that the simulation results verify the accuracy of the analytical results, thus validating the effectiveness of the system analysis. Moreover, two curves in Fig. 3 representing different values of  $Y_{th}$  are plotted, namely  $Y_{th} = 1.0$  and  $Y_{th} = 2.0$ . The curve corresponding to  $Y_{th} = 2.0$  is located above the curve associated with  $Y_{th} = 1.0$  due to a smaller latency threshold leading to an improved system performance. Additionally, the results for both curves reveal that the system outage probability decreases as  $\alpha$  increases. This outcome indicates that a higher value of  $\alpha$  can enhance the wireless transmission quality for the considered system.

#### 4.2. Outage probability of the system with $n > 1$ .

In this part, we perform the simulations in terms of the system outage probability with multiple relays, where  $n \in [1, 2, 3, 4, 5]$  and relay selection criterion I or II is employed. When criterion I is used, the associated experimental results are shown in Fig. 4 and Table 3. As demonstrated in Fig. 4 and Table 3, one can see that the simulation and analytical results exhibit similar values for various values of  $Y_{th}$  and  $n$ . For example, when  $Y_{th} =$

**Figure 4.** System outage probability versus relay number  $n$  and  $Y_{th}$  for criterion I.

1.0 and  $n = 1$ , the simulation result is 0.0876, while the analytical result is 0.0869, yielding a difference of only 0.0007. Similarly, when  $Y_{th} = 2.0$  and  $n = 5$ , the simulation result is 0.0001, while the analytical result is 0.0001, which is the same as each other. These findings lead to the conclusion that the simulation results validate the accuracy of the analytical results, thereby confirming the effectiveness of the system analysis on the outage probability. Moreover, the two curves in Fig. 4 are plotted representing different values of  $Y_{th}$ , namely  $Y_{th} = 1.0$  and  $Y_{th} = 2.0$ . The curve associated with  $Y_{th} = 2.0$  is positioned above the curve corresponding to  $Y_{th} = 1.0$  due to the a lower threshold. Additionally, the results for both curves reveal that the system outage probability decreases as  $n$  increases. This outcome suggests that a higher value of  $n$  can help enhance the transmission quality effectively for criterion I.

For criterion II with multiple relays, the experimental results are shown in Fig. 5 and Table 4. As shown in Fig. 5 and Table 4, one can obtain that the simulation results and analytical results demonstrate similar values for different values of  $Y_{th}$  and  $n$ . For instance, when  $Y_{th} = 1.0$  and  $n = 1$ , the simulation result is 0.0885, while the analytical result is 0.0869, resulting in a difference of

**Table 2.** Numerical outage probability with  $n = 1$  versus  $\alpha$  and  $Y_{th}$ .

Methods	$Y_{th}$	$\alpha$				
		1	2	3	4	5
Simulation	1.0	0.0885	0.0475	0.0321	0.0249	0.0207
	2.0	0.1676	0.0892	0.0625	0.0475	0.0384
Analysis	1.0	0.0869	0.0449	0.0304	0.0231	0.0187
	2.0	0.1662	0.0877	0.0599	0.0457	0.0371

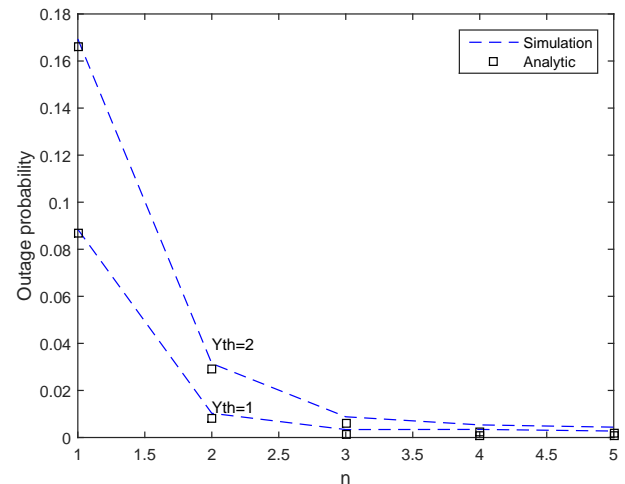
**Table 3.** Numerical outage probability versus relay number  $n$  and  $Y_{th}$  for criterion I.

Methods	$Y_{th}$	$n$				
		1	2	3	4	5
Simulation	1.0	0.0876	0.0076	0.0007	0.0001	0.0000
	2.0	0.1680	0.0275	0.0049	0.0008	0.0001
Analysis	1.0	0.0869	0.0076	0.0007	0.0001	0.0000
	2.0	0.1662	0.0276	0.0046	0.0008	0.0001

only 0.0016. Similarly, when  $Y_{th} = 2.0$  and  $n = 5$ , the simulation result is 0.0044, while the analytical result is 0.00019, resulting in a difference of only 0.0025. These observations lead to the conclusion that the simulation results validate the accuracy of the analytical results, thereby confirming the effectiveness of the system analysis on the outage probability. Moreover, the two curves in Fig. 4 are plotted representing different values of  $Y_{th}$ , namely  $Y_{th} = 1.0$  and  $Y_{th} = 2.0$ . In particular, the curve associated with  $Y_{th} = 2.0$  is positioned above the curve corresponding to  $Y_{th} = 1.0$  due to a lower threshold enhancing the system performance. In further, the results for both curves reveal that the system outage probability decreases as  $n$  increases. This outcome suggests that a higher value of  $n$  can help enhance the transmission quality effectively for criterion II.

## 5. Conclusions

In conclusion, this paper has extensively investigated multi-relay assisted IoT networks in mixed fading environments. Through the use of DF relays, data transmission has been facilitated from source to destination. The study's focal point was on mixed fading environments, particularly those characterized by distinct fading behaviors in the first-hop and second-hop relaying links. The introduction of two relay selection criteria has been pivotal in enhancing the overall network efficiency. The optimal selection criterion, which centers around identifying the most proficient relay based on dual-hop relaying links, and the sub-optimal selection criterion, which chooses the optimal relay based on the second-hop relaying link characteristics, have been provided. The evaluation of these criteria's performance involved the derivation of analytical expressions governing the system outage probability. The validity of the

**Figure 5.** System outage probability versus relay number  $n$  and  $Y_{th}$  for criterion II.

theoretical framework has been demonstrated through comprehensive simulation results. Notably, the research findings underscore the positive impact of increasing the number of relays in the network topology on enhancing network performance, even in complicated mixed fading environments.

### 5.1. Copyright

The Copyright was licensed to EAI.

### References

- [1] Z. Huang, L. Bai, X. Cheng, X. Yin, P. E. Mogensen, and X. Cai, "A non-stationary 6g V2V channel model with continuously arbitrary trajectory," *IEEE Trans. Veh. Technol.*, vol. 72, no. 1, pp. 4–19, 2023.

**Table 4.** Numerical outage probability versus relay number  $n$  and  $Y_{th}$  for criterion II.

Methods	$Y_{th}$	$n$				
		1	2	3	4	5
Simulation	1.0	0.0885	0.00.0103	0.0034	0.0034	0.0027
	2.0	0.1674	0.0295	0.0081	0.0049	0.0044
Analysis	1.0	0.0869	0.0083	0.0015	0.0010	0.0010
	2.0	0.1662	0.0289	0.0063	0.0025	0.0019

- [2] K. Sultana, K. Ahmed, B. Gu, and H. Wang, "Elastic optimization for stragglers in edge federated learning," *Big Data Mining and Analytics*, vol. 6, no. 4, pp. 404–420, 2023.
- [3] A. E. Haddad and L. Najafizadeh, "The discriminative discrete basis problem: Definitions, algorithms, benchmarking, and application to brain's functional dynamics," *IEEE Trans. Signal Process.*, vol. 71, pp. 1–16, 2023.
- [4] R. Gabrys, S. Pattabiraman, and O. Milenkovic, "Reconstruction of sets of strings from prefix/suffix compositions," *IEEE Trans. Commun.*, vol. 71, no. 1, pp. 3–12, 2023.
- [5] F. L. Andrade, M. A. T. Figueiredo, and J. Xavier, "Distributed banach-picard iteration: Application to distributed parameter estimation and PCA," *IEEE Trans. Signal Process.*, vol. 71, pp. 17–30, 2023.
- [6] Q. Wang, S. Cai, Y. Wang, and X. Ma, "Free-ride feedback and superposition retransmission over LDPC coded links," *IEEE Trans. Commun.*, vol. 71, no. 1, pp. 13–25, 2023.
- [7] Z. Xie, W. Chen, and H. V. Poor, "A unified framework for pushing in two-tier heterogeneous networks with mmwave hotspots," *IEEE Trans. Wirel. Commun.*, vol. 22, no. 1, pp. 19–31, 2023.
- [8] Y. Fang, "-ary distributed arithmetic coding for uniform -ary sources," *IEEE Trans. Inf. Theory*, vol. 69, no. 1, pp. 47–74, 2023.
- [9] M. Hellkvist, A. Özçelikkale, and A. Ahlén, "Estimation under model misspecification with fake features," *IEEE Trans. Signal Process.*, vol. 71, pp. 47–60, 2023.
- [10] Z. Xuan and K. Narayanan, "Low-delay analog joint source-channel coding with deep learning," *IEEE Trans. Commun.*, vol. 71, no. 1, pp. 40–51, 2023.
- [11] T. Ma, Y. Xiao, X. Lei, W. Xiong, and M. Xiao, "Distributed reconfigurable intelligent surfaces assisted indoor positioning," *IEEE Trans. Wirel. Commun.*, vol. 22, no. 1, pp. 47–58, 2023.
- [12] R. Singh, S. Subramani, J. Du, Y. Zhang, H. Wang, Y. Miao, and K. Ahmed, "Antisocial behavior identification from twitter feeds using traditional machine learning algorithms and deep learning." *EAI Endorsed Transactions on Scalable Information Systems*, vol. 10, no. 4, pp. e17–e17, 2023.
- [13] N. Venkateswaran and S. P. Prabaharan, "An efficient neuro deep learning intrusion detection system for mobile adhoc networks," *EAI Endorsed Transactions on Scalable Information Systems*, vol. 9, no. 6, pp. e7–e7, 2022.
- [14] M. You, J. Yin, H. Wang, J. Cao, K. Wang, Y. Miao, and E. Bertino, "A knowledge graph empowered online learning framework for access control decision-making," *World Wide Web*, vol. 26, no. 2, pp. 827–848, 2023.
- [15] D. Malak and M. Médard, "A distributed computationally aware quantizer design via hyper binning," *IEEE Trans. Signal Process.*, vol. 71, pp. 76–91, 2023.
- [16] Y. Xiong, S. Sun, L. Liu, Z. Zhang, and N. Wei, "Performance analysis and bit allocation of cell-free massive MIMO network with variable-resolution adcs," *IEEE Trans. Commun.*, vol. 71, no. 1, pp. 67–82, 2023.
- [17] J. Shao, Y. Mao, and J. Zhang, "Task-oriented communication for multidevice cooperative edge inference," *IEEE Trans. Wirel. Commun.*, vol. 22, no. 1, pp. 73–87, 2023.
- [18] H. H. López and G. L. Matthews, "Multivariate goppa codes," *IEEE Trans. Inf. Theory*, vol. 69, no. 1, pp. 126–137, 2023.
- [19] Y. Sun, D. Wu, X. S. Fang, and J. Ren, "On-glass grid structure and its application in highly-transparent antenna for internet of vehicles," *IEEE Trans. Veh. Technol.*, vol. 72, no. 1, pp. 93–101, 2023.
- [20] P. Tichavský, O. Straka, and J. Duník, "Grid-based bayesian filters with functional decomposition of transient density," *IEEE Trans. Signal Process.*, vol. 71, pp. 92–104, 2023.
- [21] C. Zeng, J. Wang, C. Ding, M. Lin, and J. Wang, "MIMO unmanned surface vessels enabled maritime wireless network coexisting with satellite network: Beamforming and trajectory design," *IEEE Trans. Commun.*, vol. 71, no. 1, pp. 83–100, 2023.
- [22] Q. Li, R. Gan, J. Liang, and S. J. Godsill, "An adaptive and scalable multi-object tracker based on the non-homogeneous poisson process," *IEEE Trans. Signal Process.*, vol. 71, pp. 105–120, 2023.
- [23] F. Hu, Y. Deng, and A. H. Aghvami, "Scalable multi-agent reinforcement learning for dynamic coordinated multipoint clustering," *IEEE Trans. Commun.*, vol. 71, no. 1, pp. 101–114, 2023.
- [24] H. Hui and W. Chen, "Joint scheduling of proactive pushing and on-demand transmission over shared spectrum for profit maximization," *IEEE Trans. Wirel. Commun.*, vol. 22, no. 1, pp. 107–121, 2023.
- [25] W. Yu, Y. Xi, X. Wei, and G. Ge, "Balanced set codes with small intersections," *IEEE Trans. Inf. Theory*, vol. 69, no. 1, pp. 147–156, 2023.
- [26] Z. Zhang, Z. Shi, and Y. Gu, "Ziv-zakai bound for doas estimation," *IEEE Trans. Signal Process.*, vol. 71, pp. 136–149, 2023.
- [27] S. Guo and X. Zhao, "Multi-agent deep reinforcement learning based transmission latency minimization for delay-sensitive cognitive satellite-uav networks," *IEEE Trans. Commun.*, vol. 71, no. 1, pp. 131–144, 2023.

- [28] X. Fang, W. Feng, Y. Wang, Y. Chen, N. Ge, Z. Ding, and H. Zhu, "Noma-based hybrid satellite-uav-terrestrial networks for 6g maritime coverage," *IEEE Trans. Wirel. Commun.*, vol. 22, no. 1, pp. 138–152, 2023.
- [29] S. Mosharafian and J. M. Velni, "Cooperative adaptive cruise control in a mixed-autonomy traffic system: A hybrid stochastic predictive approach incorporating lane change," *IEEE Trans. Veh. Technol.*, vol. 72, no. 1, pp. 136–148, 2023.
- [30] X. Niu and E. Wei, "Fedhybrid: A hybrid federated optimization method for heterogeneous clients," *IEEE Trans. Signal Process.*, vol. 71, pp. 150–163, 2023.
- [31] R. Yang, Z. Zhang, X. Zhang, C. Li, Y. Huang, and L. Yang, "Meta-learning for beam prediction in a dual-band communication system," *IEEE Trans. Commun.*, vol. 71, no. 1, pp. 145–157, 2023.
- [32] Z. Yang, F. Li, and D. Zhang, "A joint model extraction and data detection framework for IRS-NOMA system," *IEEE Trans. Signal Process.*, vol. 71, pp. 164–177, 2023.
- [33] T. Zhang, K. Zhu, S. Zheng, D. Niyato, and N. C. Luong, "Trajectory design and power control for joint radar and communication enabled multi-uav cooperative detection systems," *IEEE Trans. Commun.*, vol. 71, no. 1, pp. 158–172, 2023.
- [34] M. Zaher, Ö. T. Demir, E. Björnson, and M. Petrova, "Learning-based downlink power allocation in cell-free massive MIMO systems," *IEEE Trans. Wirel. Commun.*, vol. 22, no. 1, pp. 174–188, 2023.
- [35] N. Zhang, M. Tao, J. Wang, and F. Xu, "Fundamental limits of communication efficiency for model aggregation in distributed learning: A rate-distortion approach," *IEEE Trans. Commun.*, vol. 71, no. 1, pp. 173–186, 2023.
- [36] X. Yue, J. Xie, Y. Liu, Z. Han, R. Liu, and Z. Ding, "Simultaneously transmitting and reflecting reconfigurable intelligent surface assisted NOMA networks," *IEEE Trans. Wirel. Commun.*, vol. 22, no. 1, pp. 189–204, 2023.
- [37] M. Salman and M. K. Varanasi, "Diamond message set groupcasting: From an inner bound for the DM broadcast channel to the capacity region of the combination network," *IEEE Trans. Inf. Theory*, vol. 69, no. 1, pp. 223–237, 2023.
- [38] Z. Feng, M. Yu, S. A. Evangelou, I. M. Jaimoukha, and D. Dini, "Mu-synthesis PID control of full-car with parallel active link suspension under variable payload," *IEEE Trans. Veh. Technol.*, vol. 72, no. 1, pp. 176–189, 2023.
- [39] S. Khirirat, X. Wang, S. Magnússon, and M. Johansson, "Improved step-size schedules for proximal noisy gradient methods," *IEEE Trans. Signal Process.*, vol. 71, pp. 189–201, 2023.
- [40] C. Chaieb, F. Abdelkefi, and W. Ajib, "Deep reinforcement learning for resource allocation in multi-band and hybrid OMA-NOMA wireless networks," *IEEE Trans. Commun.*, vol. 71, no. 1, pp. 187–198, 2023.
- [41] Z. Song, J. An, G. Pan, S. Wang, H. Zhang, Y. Chen, and M. Alouini, "Cooperative satellite-aerial-terrestrial systems: A stochastic geometry model," *IEEE Trans. Wirel. Commun.*, vol. 22, no. 1, pp. 220–236, 2023.